Life Sciences 84 (2009) 428–436

Contents lists available at ScienceDirect

Life Sciences

journal homepage: www.elsevier.com/locate/lifescie

Antioxidative effect of the herbal remedy Qin Huo Yi Hao and its active component tetramethylpyrazine on high glucose-treated endothelial cells

Yingxiu Kang [a], Minghua Hu [b], Yanhui Zhu [b], Xin Gao [a,*], Ming-Wei Wang [b,*]

[a] Endocrinology and Metabolism, Zhongshan Hospital, Fudan University, Shanghai, China
[b] The National Center for Drug Screening and State Key Laboratory of Drug Research, Shanghai Institute of Materia Medica, Chinese Academy of Science, Shanghai, China

ARTICLE INFO

Article history:
Received 24 July 2008
Accepted 14 January 2009

Keywords:
Traditional Chinese medicine
Oxidative stress
Endothelial cells
Tetramethylpyrazine (TMP)
Nitric oxide (NO)

ABSTRACT

Aims: This study was designed to gain insights into the antioxidant mechanism of a Chinese herbal remedy, Qing Huo Yi Hao (QHYH), and its active components against oxidative stress induced by high glucose in endothelial cells.
Main methods: Effects of QHYH on reactive oxygen species (ROS) production and nitric oxide (NO) generation were measured with the fluorescent markers H_2DCF-DA and DAF-FM DA, respectively. Phosphorylation of Akt (protein kinase B)/eNOS (endothelial nitric oxide synthase) and uncoupling protein 2 (UCP2) expression were studied by Western blot techniques. Influences of QHYH and one of the active components (tetramethylpyrazine, TMP) on UCP2 expression were subsequently evaluated by quantitative real-time reverse transcription–polymerase chain reaction. Using RNA interference techniques, the involvement of UCP2 in high glucose-induced ROS production in mouse brain microvascular (bEnd.3) cells and its correlation with the antioxidant effect of QHYH were further assessed.
Key findings: Our results showed that QHYH could protect endothelial cells from high glucose-induced damages, such as ROS production, down-regulation of Akt/eNOS phosphorylation and reduction of NO generation. The protective properties of QHYH were partially attributed to UCP2 mRNA/protein expression, because silence of UCP2 gene by siRNAs (small interfering RNAs) abolished such effects. A total of 28 extracts and 11 active components isolated from QHYH were functionally analyzed. Of which, TMP displayed comparable antioxidant and endothelial protective effects as QHYH.
Significance: All of the data, taken together, point to some therapeutic potential of QHYH and TMP for vascular complications of diabetes.

Introduction

Vascular complications are the principal causes of morbidity and mortality in patients with diabetes mellitus (Eckel et al. 2002). Cardiovascular disease accounts for more than 50% of all deaths in diabetic patients (Cooper and Johnston 2000). Endothelial dysfunction characterized by a decrease in the bioavailability of endothelial nitric oxide (NO) has been observed in individuals with hyperglycemia and may be a critical and initiating factor in the pathogenesis of diabetic vascular complications. An underlying mechanism for endothelial dysfunction is the enhanced generation of endothelial reactive oxygen species (ROS). Excessive ROS is able to react with endothelial cell protective factor NO and cause damages to endothelial cells, by means of decreasing NO bioactivity and producing a toxic oxidant, peroxynitrite (Ceriello 2003).

Hyperglycemia can induce oxidative stress via several mechanisms, including glucose autoxidation (Nishikawa et al. 2000), AGE formation (Basta et al. 2005; Yamagishi et al. 2008; Su et al. 2008) and polyol pathway activation (Jay et al. 2006). At the cellular level, potential sources of endothelial ROS that are implicated in disease processes include mitochondria, NADPH oxidases, xanthine oxidase (XO), etc., among which, mitochondrial respiratory chain is believed to be a major site of ROS generation (Cave et al. 2006; Newsholme et al. 2007; Paravicini and Touyz 2008). Uncoupling protein 2 (UCP2) resides in the inner mitochondrial membrane and catalyzes a proton conductance that dissipates the proton electrochemical gradient built up by the respiratory chain. Recent studies indicate that (i) UCP2 is involved in the control of mitochondrial membrane potential and ROS generation (Teshima et al. 2003; Chevillotte et al. 2007); and (ii) genetic ablation of UCP2 produces more ROS in endothelial cells (Lee et al. 2005).

"Causal" antioxidant therapy represents a new and attractive strategy for the treatment of vascular complications in diabetes (Ceriello 2003). Vitamin E, a classic antioxidant, could scavenge already-formed toxic oxidation products, but failed to show beneficial effects on diabetic complications. Qing Huo Yi Hao (QHYH) is an herbal remedy derived

* Corresponding authors. Gao is to be contacted at Tel.: +86 21 64439025; fax: +86 21 64037269. Wang, Tel.: +86 21 50800598; fax: +86 21 50800721.
E-mail addresses: gao.xin@zs-hospital.sh.cn (X. Gao), wangmw@mail.shcnc.ac.cn (M.-W. Wang).

0024-3205/$ – see front matter © 2009 Elsevier Inc. All rights reserved.
doi:10.1016/j.lfs.2009.01.003

from traditional Chinese medicine (TCM) to treat diabetic vascular complications. We have previously reported that QHYH was able to decrease urinary microalbumin excretion in type 2 diabetic patients and promote microvascular endothelial cell growth in high glucose medium, suggesting that it has beneficial effects on diabetic vascular complications and can protect endothelial cells from damages caused by high glucose environment (Yu et al. 2004; Zhang et al. 2005).

The present study was therefore conducted with an attempt to elucidate the potential mechanism(s) responsible for the therapeutic benefits of QHYH, including effects on ROS production, NO generation and phosphorylation of Akt and eNOS in mouse brain microvascular (bEnd.3) cells. The involvement of UCP2 in high glucose-induced ROS production and its correlation with the antioxidant effect of QHYH on bEnd.3 cells were also investigated. Since QHYH is a complex mixture containing hundreds of constituents with different chemical structures and only a handful of them are responsible for the pharmacological activities observed, bioassay-guided natural product chemistry methods were employed to extract and isolate active components associated with the antioxidant properties of QHYH.

Materials and methods

Chemistry

A mixture of 8 herbal plants contained in QHYH was boiled in distilled water (2000 ml) for 6 h to give 300 ml crude product, which was mixed with 95% ethanol (1500 ml) and left at room temperature for 72 h. Supernatant was then collected and concentrated to 400 ml.

The above extract was partitioned 3 times with 400 ml ethyl acetate and 400 ml n-butyl alcohol, respectively, which delivered 3 fractions. Part of the EtOAc fraction (3.2 g) was purified using column chromatography on silica gel by elution with $CHCl_3$. The resultant 12 subfractions were analyzed by TLC and 3 of them showed bioactivity. Successive flash chromatography of subfraction 1 using EtOAC and petroleum ether as binary mixture of increasing polarity yielded E1-f1-2 (104 mg; 4′-hydroxyacetophenone or parahydroxy acetophenone) and E1-f1-5 (163 mg; hesperidin). Similar chromatography of subfraction 4 eluted with EtOAc and $CHCl_3$ yielded E1-f4-3 (134 mg; tetramethylpyrazine, Fig. 1), and of subfraction 7 with CCl_4 and AcOEt delivered E1-f7-2 (179 mg; ferulic acid).

Part of the n-BuOH fraction (7.8 g) was subject to chromatography using MeOH and 3 subfractions were obtained with 1 demonstrating bioactivity. E2-f2-2 (207 mg; puerarin), E2-f2-3 (57 mg; crocin) and E2-f2-4 (33 mg; astragalus saponin I) were purified from a silica gel column with $CHCL_3$ and 5%–95% MeOH.

Part of the EtOH fraction (35.7 g) was separated by MCI and eluted with H_2O and EtOH. Of the 10 subfractions obtained, only 2 displayed bioactivity. E3-f2-2 (203 mg; chlorogenic acid), E3-f4-2 (247 mg; geniposide), E3-f4-3 (126 mg; deacetylasperulosidic acid methyl ester) and E3-f4-4 (176 mg; geniposide gentiobioside) were isolated subsequently using CH_2Cl_2 and MeOH.

The structures of 11 isolated compounds were confirmed by ^1H NMR, ^{13}C NMR and EI–MS.

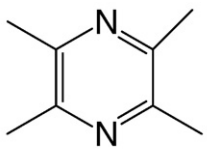

Tetramethylpyrazine

Fig. 1. Chemical structure of tetramethylpyrazine.

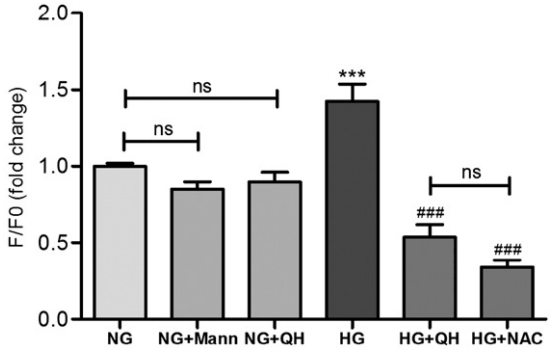

Fig. 2. Effect of QHYH on ROS production in bEnd.3 cells. After loading with H_2DCF-DA, cells were treated separately with 5.6 mM glucose (NG), 5.6 mM glucose plus 19.2 mM mannitol (NG + Mann), 5.6 mM glucose plus QHYH (1:100) (NG + QH), 25 mM glucose (HG), 25 mM glucose plus QHYH (1:100) (HG + QH), or 25 mM glucose plus N-acetylcysteine (HG + NAC) for 60 min before measurement of changes in fluorescence intensity. F0 represents baseline fluorescence and *F* depicts fluorescence after treatment. Data shown are fold changes compared to control values (NG). ***$P<0.001$ *vs.* NG; $^{###}P<0.001$ *vs.* HG; ns, not statistically significant.

Cell culture

Immortalized bEnd.3 cell line was generously provided by Dr. Huiming Jin (Fudan University, Shanghai, China). Cells were cultured in low glucose (5.6 mM)-Dulbecco's modified Eagle's medium (DMEM) (Gibco BRL, Grand Island, NY, USA) supplemented with 10% fetal bovine serum (FBS) at 37 °C in a humidified atmosphere of 5% CO_2.

Human aortic endothelial cells (HAEC) and human umbilical vein endothelial cells (HUVEC) were purchased from Cascade Biologics, Inc. (Portland, OR, USA) and maintained at 37 °C under 5% CO_2 in medium 200 supplemented with low-serum growth supplement (20 μl/ml; Cascade Biologics). All experiments were performed in cells at passages 6–8.

Table 1
Effects of 11 natural compounds isolated from QHYH on ROS production in bEnd.3 cells

		% Inhibition			
		1 μM	3 μM	10 μM	30 μM
Geniposide	NG	2.9 ± 2.8	2.4 ± 2.3	2.5 ± 1.0	11.5 ± 2.5
	HG	3.7 ± 1.7	9.3 ± 2.4	5.5 ± 2.1	10.0 ± 1.8
Astragalus saponin I	NG	6.3 ± 0.7	23.6 ± 1.3***	34.0 ± 3.6***	30.7 ± 3.2***
	HG	26.3 ± 1.7$^{###}$	49.8 ± 0.9$^{###}$	41.5 ± 3.8$^{###}$	44.9 ± 1.2$^{###}$
Puerarin	NG	3.1 ± 0.9	NA	NA	NA
	HG	3.6 ± 3.8	8.9 ± 1.8	28.1 ± 4.6$^{###}$	13.8 ± 2.7
Hesperidin	NG	9.0 ± 4.2	22.8 ± 2.2**	24.8 ± 3.0**	38.8 ± 2.6***
	HG	NA	14.0 ± 4.0	11.5 ± 8.4	9.7 ± 6.6
Crocin	NG	NA	36.9 ± 3.0***	76.3 ± 1.6***	84.7 ± 5.8***
	HG	17.8 ± 5.3$^{#}$	40.1 ± 7.1$^{###}$	65 ± 1.3$^{###}$	71.3 ± 3.6$^{###}$
Tetramethylpyrazine	NG	14.0 ± 6.6***	16.4 ± 6.9***	17.3 ± 6.8***	22.7 ± 3.7**
	HG	15.1 ± 4.1$^{###}$	34.4 ± 5.1$^{###}$	45.9 ± 8.4$^{###}$	59.3 ± 7.5$^{###}$
Ferulic acid	NG	59.0 ± 1.5***	66.6 ± 1.7***	76.6 ± 1.8***	89.1 ± 2.1***
	HG	63.2 ± 3.0$^{###}$	76.1 ± 3.8$^{###}$	64.6 ± 2.2$^{###}$	74.7 ± 1.0$^{###}$
Chlorogenic acid	NG	53.8 ± 3.6***	75.2 ± 1.2***	89.7 ± 2.6***	89.9 ± 2.5***
	HG	43.6 ± 4.2$^{##}$	44.1 ± 3.6$^{###}$	71.1 ± 7.5$^{###}$	70.2 ± 9.0$^{###}$
Parahydroxy acetophenone	NG	NA	0.9 ± 3.3	15.7 ± 2.9**	39.1 ± 2.1***
	HG	21.5 ± 2.3$^{##}$	16.8 ± 4.3$^{###}$	20.8 ± 1.2$^{###}$	49.9 ± 1.5$^{###}$
Deacetylasperulosidic acid methyl ester	NG	NA	4.6 ± 1.8	14.8 ± 3.6*	33.0 ± 0.8***
	HG	21.1 ± 2.3$^{##}$	21.9 ± 5.5$^{##}$	32.8 ± 3.6$^{###}$	51.9 ± 5.7$^{###}$
Genipin gentiobioside	NG	15.5 ± 1.8	8.3 ± 2.5	11.5 ± 2.4	11.2 ± 6.0
	HG	27.5 ± 1.5$^{###}$	36.8 ± 2.8$^{###}$	30.3 ± 3.9$^{###}$	47.2 ± 1.1$^{###}$

% Inhibition = $[(F/F0)_{\text{treated group}} - (F/F0)_{\text{control group}}] / (F/F0)_{\text{control group}} \times 100$. NG, normal glucose; HG, high glucose.
*, ** and *** stand for *P* values less than 0.05, 0.01 and 0.001, respectively, compared to normal glucose medium. $^{#}$, $^{##}$ and $^{###}$ stand for *P* values less than 0.05, 0.01 and 0.001, respectively, compared to high glucose treatment. NA, not active.

Table 2
Effect of 11 natural compounds isolated from QHYH on ROS production in HUVEC cells

		% Inhibition			
		1 μM	3 μM	10 μM	30 μM
Geniposide	NG	36.4 ± 6.3	37.0 ± 5.7	32.4 ± 5.6	29.4 ± 3.8
	HG	18.1 ± 6.8	24.6 ± 9.5	43.1 ± 4.1$^{\#}$	56.3 ± 3.1$^{\#\#}$
Astragalus saponin I	NG	35.6 ± 2.4**	24.1 ± 2.0	27.7 ± 4.1*	24.5 ± 1.1*
	HG	NA	NA	8.5 ± 8.3	NA
Puerarin	NG	23.0 ± 1.4	17.2 ± 2.6	19.4 ± 2.1	18.6 ± 2.4
	HG	20.0 ± 5.8	15.1 ± 6.1$^{\#}$	14.2 ± 5.0	19.0 ± 3.7
Hesperidin	NG	NA	NA	NA	NA
	HG	NA	26.4 ± 3.9	28.6 ± 4.1	28.7 ± 15.3
Crocin	NG	40.8 ± 3.5***	56.5 ± 0.6***	85.9 ± 2.6***	88.0 ± 0.9***
	HG	55.4 ± 4.2$^{\#\#\#}$	72.9 ± 1.2$^{\#\#\#}$	84.1 ± 3.7$^{\#\#\#}$	86.1 ± 2.3$^{\#\#\#}$
Tetramethylpyrazine	NG	3.8 ± 3.2	32.3 ± 3.1 ***	37.1 ± 1.4***	40.2 ± 0.9***
	HG	37.0 ± 3.7$^{\#\#\#}$	47.8 ± 2.7 $^{\#\#\#}$	51.5 ± 3.7$^{\#\#\#}$	58.8 ± 1.7$^{\#\#\#}$
Ferulic acid	NG	5.2 ± 5.3	66.9 ± 3.7***	76.1 ± 7.6***	67.6 ± 3.0***
	HG	39.2 ± 5.6$^{\#\#\#}$	59.2 ± 4.9$^{\#\#\#}$	80.3 ± 3.1$^{\#\#\#}$	77.7 ± 1.2$^{\#\#\#}$
Chlorogenic acid	NG	38.3 ± 5.5***	54.5 ± 2.1***	55.8 ± 2.8***	55.7 ± 1.3***
	HG	25.6 ± 0.7$^{\#\#\#}$	36.6 ± 2.0$^{\#\#\#}$	44.38 ± 1.0$^{\#\#\#}$	64.8 ± 1.1$^{\#\#\#}$
Parahydroxy acetophenone	NG	NA	1.5 ± 0.2	10.9 ± 2.3	20.9 ± 1.1***
	HG	9.6 ± 3.9 $^{\#\#}$	8.5 ± 2.7$^{\#\#}$	19.2 ± 4.6$^{\#\#}$	34.4 ± 2.5$^{\#\#\#}$
Deacetylasperulosidic acid methyl ester	NG	15.6 ± 3.5*	14.6 ± 4.7*	27.7 ± 1.6***	37.4 ± 2.8***
	HG	17.7 ± 2.4	25.0 ± 6.4	35.0 ± 1.3$^{\#\#}$	59.8 ± 2.8$^{\#\#\#}$
Genipin gentiobioside	NG	3.0 ± 1.7	20.5 ± 0.7**	34.7 ± 0.9***	37.8 ± 2.8***
	HG	19.4 ± 2.0$^{\#}$	31.2 ± 3.4$^{\#\#}$	33.9 ± 2.6$^{\#\#}$	35.6 ± 3.0$^{\#\#}$

% Inhibition = $[(F/F0)_{\text{treated group}} - (F/F0)_{\text{control group}}] / (F/F0)_{\text{control group}} \times 100$. NG, normal glucose; HG, high glucose.
*, ** and *** stand for P values less than 0.05, 0.01 and 0.001, respectively, compared to normal glucose medium. $^{\#}$, $^{\#\#}$ and $^{\#\#\#}$ stand for P values less than 0.05, 0.01 and 0.001, respectively, compared to high glucose treatment. NA, not active.

For NO and ROS measurements cells were cultured in 96-well plates and for Western blot analysis in 60 mm culture dishes (Corning Inc., Corning, NY, USA). Prior to each experiment, cells were starved overnight in low glucose-DMEM containing 1% bovine serum albumin (BSA).

Measurement of ROS production

To evaluate ROS production by bEnd.3 cells, the membrane-permeable indicator 2′,7′-dichlorodihydrofluorescein diacetate (H_2DCF-DA) (Invitrogen, Carlsbad, CA, USA) was employed. The cells were loaded with 2 μM H_2DCF-DA in serum-free low glucose-DMEM at 37 °C for 30 min and then washed twice with phosphate buffered saline (PBS). They were then treated with various preparations derived from QHYH for 60 min. H_2DCF-DA fluorescence was monitored with a FlexSstation II^{384} fluorometric imaging plate reader (Molecular Devices, Sunnyvale, CA USA) at an excitation wavelength of 488 nm and an emission wavelength of 525 nm. ROS was determined by comparing the changes in fluorescence intensity with that of the baseline (F/F0).

Determination of NO production

To assess NO production by endothelial cells (bEnd.3, HUVEC and HAEC), the membrane-permeable indicator diaminofluorescein (DAF-FM) diacetate (Invitrogen) was used (Kojima et al. 1999). This probe is converted by intracellular esterases to DAF-FM, which reacts with NO to form a green fluorescent product. DAF-FM has been reported to be useful for detection of NO in living cells (Itoh et al. 2000; Strijdom et al. 2004). The endothelial cells were loaded with 2 μM DAF-FM diacetate in serum-free low glucose-DMEM supplemented with 100 μM L-arginine (pH 7.4) at 37 °C for 30 min, washed twice with PBS, and incubated with DAF-FM diacetate-free low glucose-DMEM for an additional 20 min for de-esterification of the indicator. The cells were then treated with various preparations derived from QHYH for 60 min. DAF-FM fluorescence was measured by FlexStation II^{384} (Molecular Devices) at an excitation wavelength of 480 ± 10 nm and an emission wavelength of 510 ± 10 nm. Free cytosolic NO was determined by comparing the changes in fluorescence intensity with that of the baseline (F/F0).

Real-time PCR

Total RNA was extracted from bEnd.3 cells using RNeasy Mini Kit (QIAGEN, Hilden, Germany). One μg of the total RNA was reversely transcribed in a 20 μl volume using oligo (dT) primers, with enzyme and buffer supplied in the cDNA First Strand Synthesis kit (MBI Fermentas, Hanover, MD, USA). Quantitative real-time PCR reactions were performed on an RT-Cycler™ (CapitalBio Co., Ltd., Beijing, China) using the following primers:

β-actin forward: 5′-AGAGGGAAATCGTGCGTGAC-3′;
β-actin reverse: 5′-TGCCACAGGATTCCATACCC-3′;
UCP2 forward: 5′-GGTCCACGCAGCCTCTACAATG-3′;
UCP2 reverse: 5′-AGA AGTGAAGTGGCAAGGGAGGTC-3′.

For real-time PCR, SYBR Green QPCR Master Mix (Toyobo, Osaka, Japan) was used. The final volume of the reaction was 20 μl containing 1 μl reverse transcript (RT) sample, 10 μl QPCR Master Mix, 0.4 μl each primer (10 μM stock solution), and 8.2 μl double distilled water. Thermal cycling profile consisted of a pre-incubation step at 95 °C for 3 min, followed by 40 cycles of denaturation (94 °C, 30 s), annealing (57 °C, 30 s), and extension (72 °C, 30 s). Final PCR products were subjected to graded temperature-dependent dissociation to verify that only one product was amplified. Reactions with no RT sample and no template were included as negative controls. Relative quantitative evaluation of target gene levels was performed by the comparative CT (cycle threshold) method (Livak and Schmittgen 2001) and performed in triplicates.

Western blot analysis

bEnd.3 cells were seeded onto 6-well plates and cultured to 80% confluence. After starved with low glucose-DMEM containing 1% BSA overnight, they were treated with various preparations derived from QHYH. After removal of medium, cells were washed twice with ice-cold PBS, lysed in cell lysis buffer [20 mM Tris pH7.5, 150 mM NaCl, 1% Triton X-100, 2.5 mM sodium pyrophosphate, 1 mM EDTA, 1% Na_3VO_4, 0.5 μg/ml leupeptin, 1 mM phenylmethanesulfonyl fluoride (PMSF)],

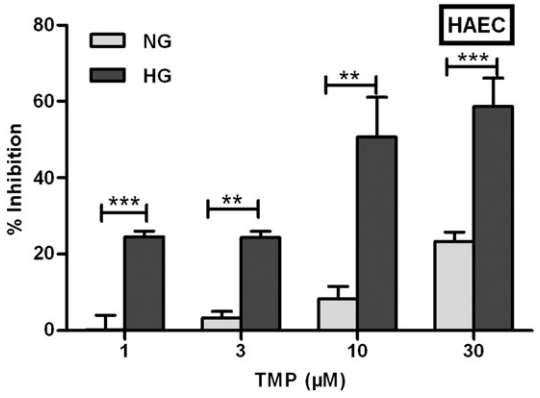

Fig. 3. Effect of TMP on ROS production in HAEC cells. After loading with H_2DCF-DA, cells were treated separately with 5.6 mM glucose (NG), TMP (10 μM), 25 mM glucose (HG), or HG plus TMP (10 μM) (HG + TMP) for 60 min before measurement of changes in fluorescence intensity. F0 represents baseline fluorescence and F depicts fluorescence after treatment. % Inhibition = $[(F/F0)_{\text{treated group}} - (F/F0)_{\text{control group}}] / (F/F0)_{\text{control group}} \times 100$. **$P$<0.01, ***$P$<0.001; NG, normal glucose, HG, high glucose.

and centrifuged at 12,000 ×*g* for 20 min at 4 °C. The supernatant was collected and used for analysis. Protein concentration was determined using a bicinchoninic acid assay (Beyotime Biotechnology, Haimen, China). The protein sample (20 μg) was heated at 100 °C for 5 min in SDS sample buffer and electrophoresis was performed on 10% SDS–PAGE gels before transferring onto nitrocellulose transfer membranes (Ameresco, Solon, OH, USA) at 350 mA for 2 h. Thereafter, the membrane was incubated with Tris-buffered saline (TBS) buffer containing 10% nonfat dry milk for 1 h at room temperature and then incubated with rabbit polyclonal antibodies against UCP2 (1:500) (Biolegend, San Diego, CA, USA), eNOS (1:500), phospho-eNOS (1:250), Akt (1:1000), and phospho-Akt (1:1000) (Cell Signaling Technology, Danvers, MA, USA) at 4 °C overnight. Following three 10 min washing in TBST (TBS containing 0.1% Tween 20), membranes were incubated for 1 h at room temperature with a horseradish peroxidase-conjugated anti-rabbit secondary antibody (Cell Signaling Technology) at 1:1000 in blocking solution (TBS containing 10% nonfat dry milk). The membrane was washed with TBST three times (10 min each) and the

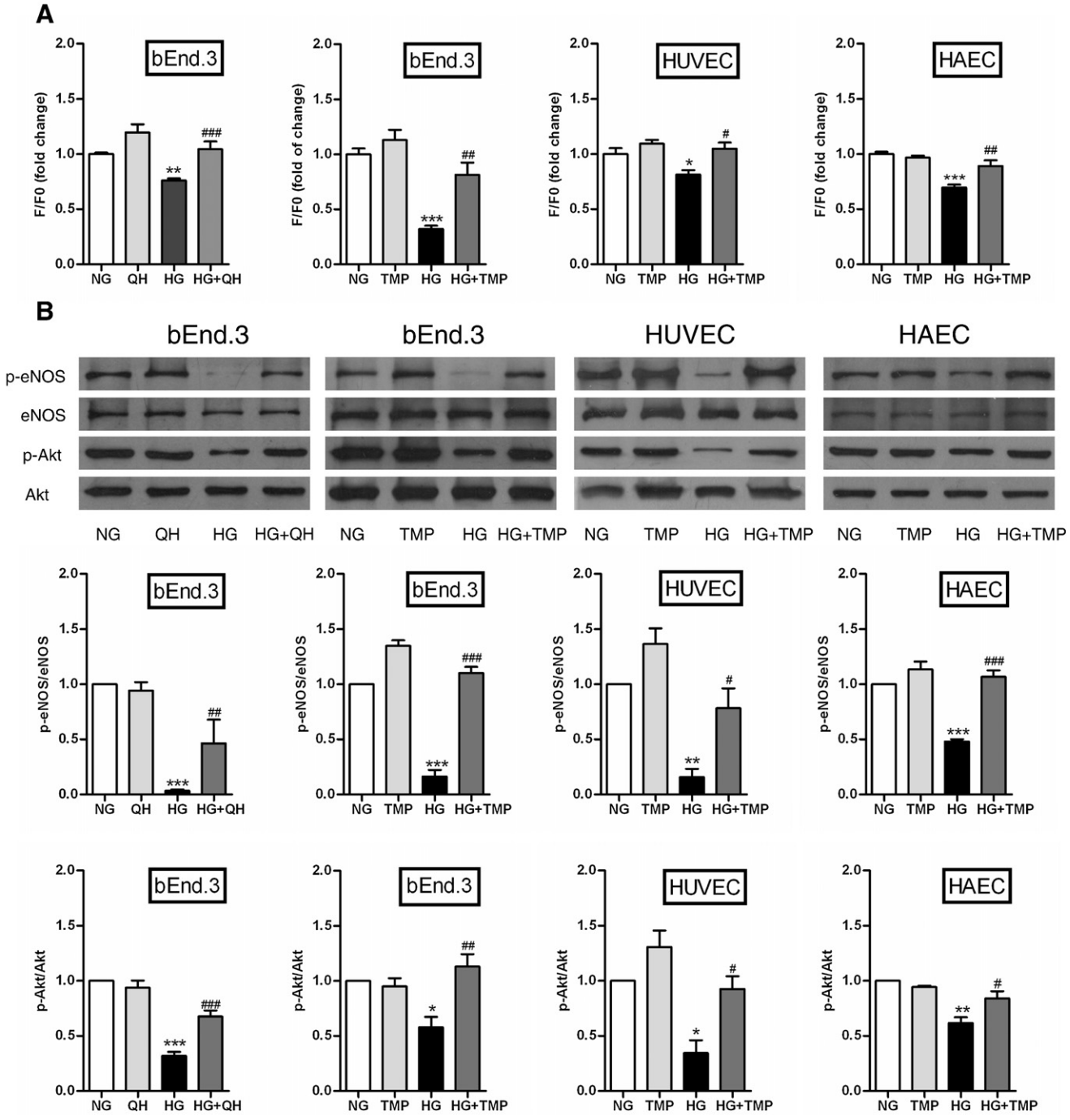

Fig. 4. Effects of QHYH and TMP on NO generation and eNOS/Akt phosphorylation in endothelial cells. (A) After loading DAF-FM diacetate, cells were treated, respectively, with 5.6 mM glucose (NG), QHYH (1:100), TMP (10 μM), 35 mM glucose (HG), HG plus QHYH (1:100) (HG + QH) or HG plus TMP (10 μM) (HG + TMP) for 60 min before measurement of changes in fluorescence intensity. F0 represents baseline fluorescence and *F* depicts fluorescence after treatment. (B) Western blotting of Akt and eNOS phosphorylation. bEnd.3 cells were treated separately with NG, QHYH, TMP, HG, HG plus QHYH or HG plus TMP for 48 h. Phosphorylation of eNOS (Ser-1177) and Akt (Ser-473) were determined with Western blotting techniques. Data shown are fold changes compared to control values (NG). $^{*}P<0.05$ *vs.* NG, $^{**}P<0.01$ *vs.* NG, $^{***}P<0.001$ *vs.* NG; $^{\#}P<0.05$ *vs.* HG, $^{\#\#}P<0.01$ *vs.* HG, $^{\#\#\#}P<0.001$ *vs.* HG.

signal was visualized by a brief incubation with the Phototope(R)-HRP Western Blot Detection System (Cell Signaling Technology). To normalize the gel loading, the membrane was also probed with a polyclonal antibody against β-actin (1:1000) (Cell Signaling Technology). Quantitative analysis of band intensity was performed using the Quantity One imaging program (Bio-Rad, Hercules, CA, USA).

RNA interference

To study the functionality of UCP2 in bEnd.3 cells, siRNAs were employed to reduce the level of UCP2 expression. Transfection of siRNAs specifically targeting UCP2 gene or a nonspecific control (GenePharma, Shanghai, China) in bEnd.3 cells was performed using

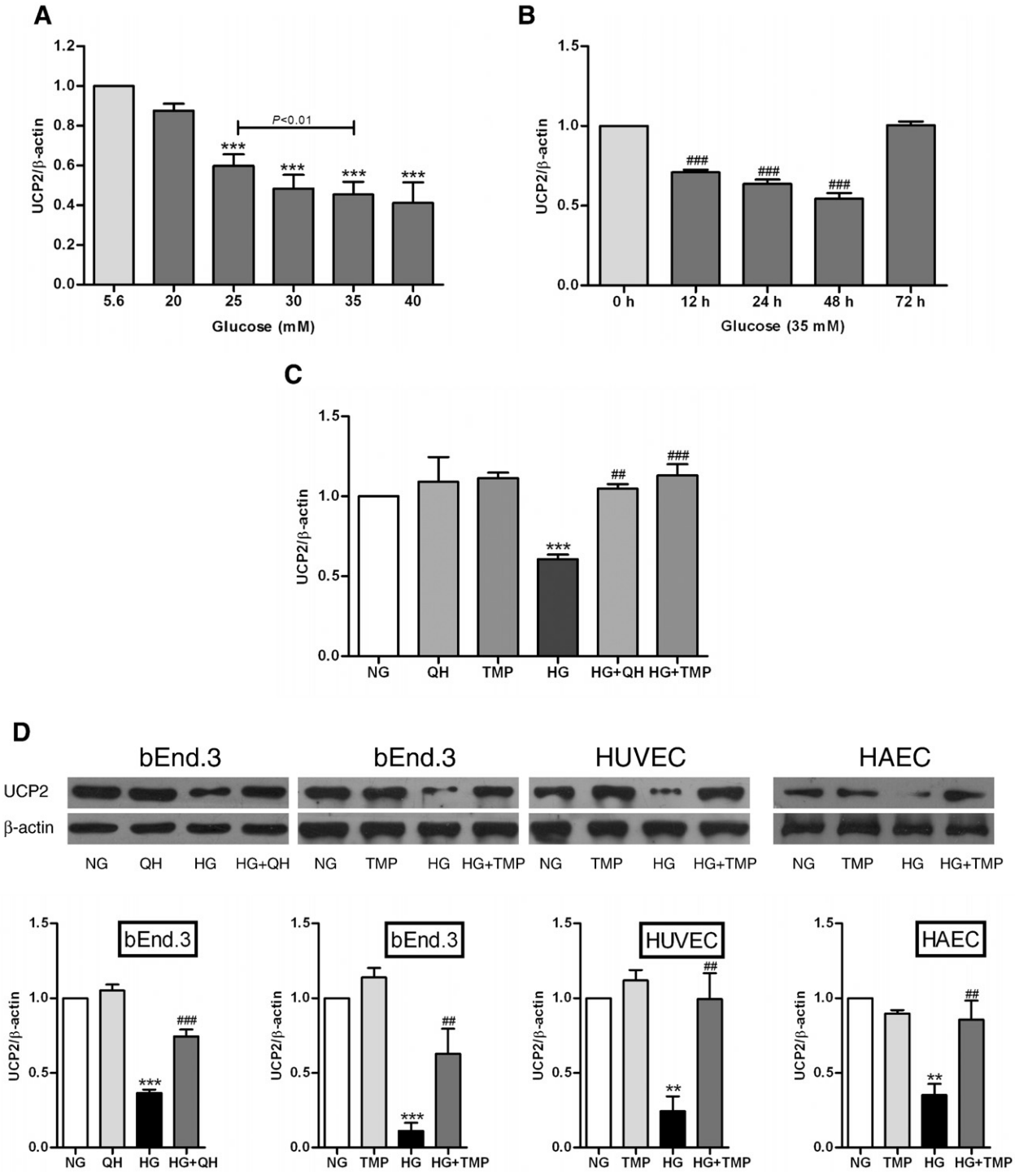

Fig. 5. High glucose-induced suppression of UCP2 mRNA/protein expression and reversal by QHYH and TMP. Dose- (A) and time-dependent (B) effects of glucose on UCP2 mRNA levels in cultured bEnd.3 cells. Cells were serum starved overnight and incubated with different concentrations of glucose (5.6 mM–40 mM) for 48 h, or with high glucose (35 mM) for 0 h–72 h. UCP2 mRNA levels were quantified by real-time PCR. $^{***}P<0.001$ *vs.* 5.6 mM glucose; $^{###}P<0.001$ *vs.* 0 h. (C) Reversal of high glucose-induced suppression of UCP2 mRNA levels by QHYH and TMP. bEnd.3 cells were treated separately with 5.6 mM glucose (NG), QHYH (1:100), TMP (10 μM), 35 mM glucose (HG), HG plus QHYH (1:100) (HG + QH), or HG plus TMP (10 μM) (HG + TMP) for 48 h. (D) Reversal of high glucose-induced suppression of UCP2 protein expression by QHYH and TMP. Endothelial cells were treated separately with NG, QHYH, TMP, HG, HG plus QH or HG plus TMP for 48 h. UCP2 protein expression was measured by Western blotting. Data shown are fold changes compared to control values (NG). $^{**}P<0.01$ *vs.* NG, $^{***}P<0.001$ *vs.* NG; $^{##}P<0.01$ *vs.* HG, $^{###}P<0.001$ *vs.* HG.

Lipofectamine 2000 reagent (Invitrogen) in serum-free medium according to the manufacturer's instructions. To determine the effectiveness of UCP2 gene knockdown by siRNAs, protein level was monitored with Western blotting. Composition of the siRNA duplexes of UCP2 oligonucleotides were 5′-CAAAGAUACUCUCCUGAAATT-3′ and 5′-UUUCAGGAGAGUAUCUUUGAT-3′, whereas the sequences of negative control siRNAs were 5′-UUCUCCGAACGUGUCACGUTT-3′ and 5′-ACGUGACACGUUCGGAGAATT-3′.

Statistical analysis

Data are expressed as means ± SEM. Statistical analysis was performed using one-way analysis of variance (ANOVA) and Student–Newman–Keul's test for individual comparisons. $P<0.05$ is considered to be statistically significant.

Results

QHYH protects bEnd.3 cells from high glucose-induced oxidative stress

Generation of intracellular ROS was measured with the probe, H_2DCF-DA, which is cell permeable and produces a fluorescent signal after oxidation by ROS. Since the efficacy of high glucose (between 25 and 40 mM) on ROS production was similar ($P>0.05$; data not shown), this concentration (25 mM) was selected in the subsequent experiments. Exposure to 25 mM D-glucose significantly increased ROS production by 42.3% compared to 5.6 mM glucose ($P<0.001$). In contrast, mannitol (used as an osmotic control) did not affect cellular ROS in bEnd.3 cells suggesting that high glucose-triggered ROS production is selective and specific. While it has no effect in normal glucose medium, QHYH at dilution of 1:100 completely abrogated high glucose-induced ROS production to a level that was well below the baseline, displaying a comparable effect as the conventional antioxidant NAC (N-acetyl-cysteine) (Fig. 2).

Active constituents isolated from QHYH reduce ROS production in endothelial cells

Chemistry efforts were made to identify and isolate antioxidant constituents from QHYH. Of the 28 extract fractions prepared, 25 exhibited various degrees of inhibition on high glucose-induced ROS production (data not shown). Subsequent separation identified 11 compounds with known structures, including geniposide, astragalus saponin I, puerarin, hesperidin, crocin, tetramethylpyrazine, ferulic acid, chlorogenic acid, parahydroxy acetophenone, deacetylasperulosidic acid methyl ester and genipin gentiobioside. Eight of them were reported previously to possess antioxidant properties (geniposide, astragalus saponin I, puerarin, hesperidin, crocin, tetramethylpyrazine, ferulic acid and chlorogenic acid). The remaining 3 (parahydroxy acetophenone, deacetylasperulosidic acid methyl ester and genipin gentiobioside) have not been implicated of such a function so far in the literature. Potential inhibition on ROS production of these 11 natural compounds were therefore evaluated in bEnd.3 (Table 1) and HUVEC cells (Table 2), and 7 of them (crocin, tetramethylpyrazine, ferulic acid, chlorogenic acid, parahydroxy acetophenone, deacetylasperulosidic acid methyl ester and genipin gentiobioside) were confirmed to exert antioxidant actions in both types of endothelial cells. The inhibitory effect of tetramethylpyrazine (TMP) on high glucose-induced ROS production was more consistent and its antioxidant feature was also demonstrable in HAEC cells (Fig. 3). The effect of TMP on ROS generated by xanthine/

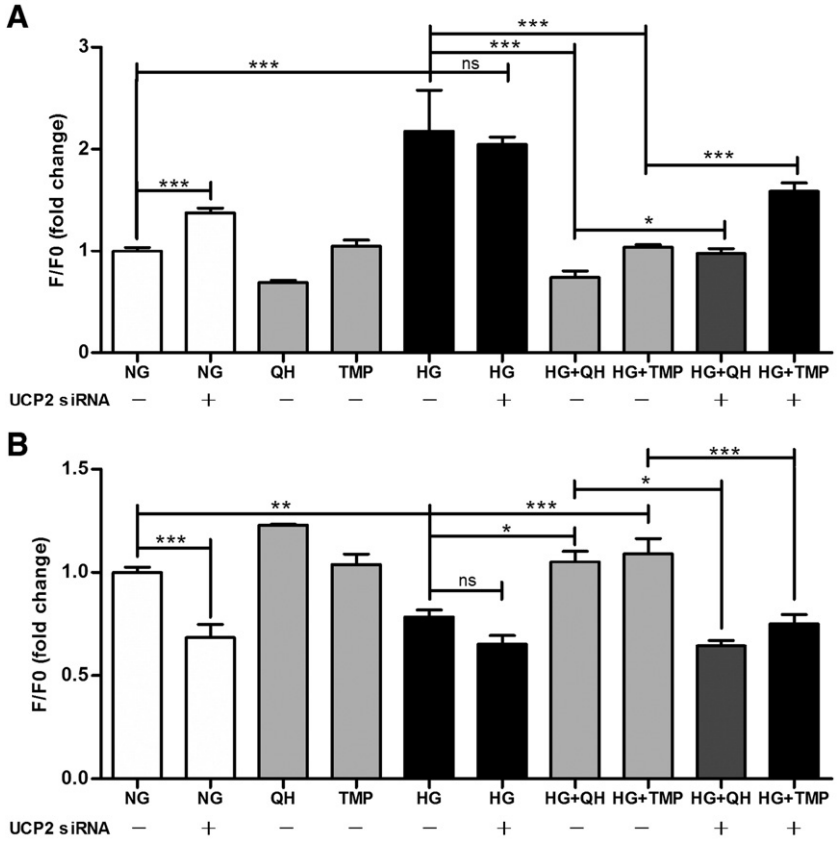

Fig. 6. Effects of UCP2 siRNA transfection on ROS generation (A), NO production (B), Akt and eNOS phosporylation (C) in bEnd.3 cells. The cells were transfected with UCP2 siRNA for 24 h followed by treatment with different regimens as indicated before measuring ROS and NO production. F0 represents baseline fluorescence and *F* depicts fluorescence after treatment. Data shown are fold changes compared to control values (NG). *$P<0.05$, **$P<0.01$ and ***$P<0.001$, ns, not statistically significant. NG, normal glucose; HG, high glucose; QH, QHYH.

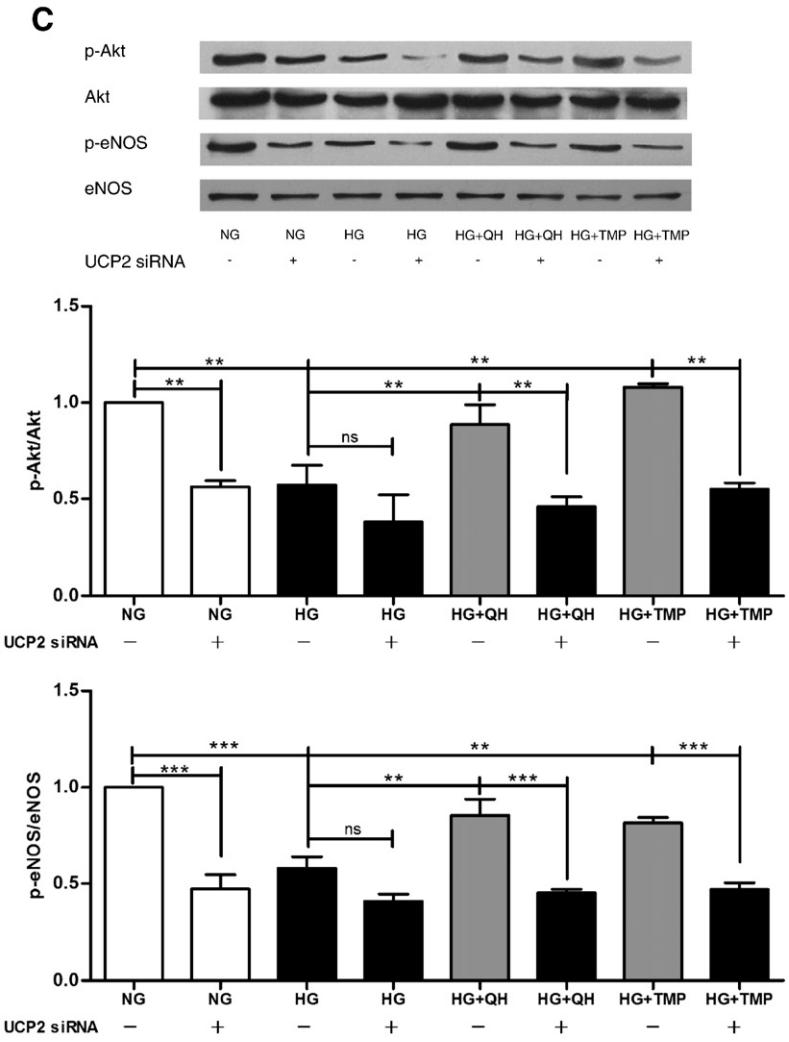

Fig. 6 (*continued*).

xanthine oxidase system was also studied. TMP did not show a direct scavenging property on ROS whereas the control compound, quercetin, acted as a scavenger in a concentration-dependent manner (data not shown). TMP was thus selected as a representative active component for subsequent parallel studies with QHYH.

QHYH and TMP reverse high glucose-induced suppression of NO generation and eNOS/Akt phosphorylation

To examine potential effects of QHYH and TMP on endothelial functions, the production of NO in bEnd.3, HUVEC and HAEC cells was determined using a fluorescent NO indicator, DAF-FM diacetate. While D-glucose inhibited NO production in bEnd.3 cells in a concentration-dependent manner, significant difference was observed only in the two highest dose groups (35 and 40 mM; data not shown). As demonstrated in Fig. 4A (1st panel), 35 mM D-glucose decreased DAF-FM fluorescence intensity by 24% compared to the control (5.6 mM glucose, $P<0.05$); co-incubation with QHYH completely reversed this trend. Such a protective property could be reproduced by TMP isolated from QHYH as it was able to abolish high glucose-induced suppression of NO production in all the three types of endothelial cells (Fig. 4A, 2nd, 3rd and 4th panel).

Phosphorylation of eNOS at residue Ser-1177 (Kobayashi et al. 2005) is an event prior to NO generation in endothelial cells. The time-course effect of 35 mM high glucose on eNOS phosphorylation in bEnd.3 cells was evaluated at different intervals between 1 and 48 h. Inhibition of eNOS phosphorylation was detectable at 1 h but was most pronounced at 48 h following addition of high glucose (Data not shown). Incubation of bEnd.3, HUVEC or HAEC cells with 35 mM D-glucose inhibited Ser-1177-eNOS phosphorylation without altering the total eNOS protein levels (Fig. 4B). This inhibitory effect of high glucose was attenuated by both QHYH (in bEnd.3 cells; from a phosphorylated/total Ser-1177-eNOS ratio of 0.03 ± 0.01 to 0.46 ± 0.22, $P<0.01$) and TMP with varying phosphorylation ratios in bEnd.3 (0.10 ± 0.01 *vs.* 1.20 ± 0.06, $P<0.001$), HUVEC (0.16 ± 0.07 *vs.* 0.78 ± 0.18, $P<0.05$) and HAEC (0.48 ± 0.02 *vs.* 1.07 ± 0.06, $P<0.001$) cells.

Since phosphorylation of eNOS at Ser-1177 is a downstream effect of the serine kinase Akt (Yang and Ming 2006), we further examined the involvement of Akt in endothelial oxidative stress under high glucose environment. Akt (Ser-473) phosphorylation in bEnd.3 cells was markedly reduced following high glucose treatment, but the trend was reversed after addition of QHYH (from 0.32 ± 0.04 to 0.68 ± 0.05, $P<0.01$) (Fig. 4B). This effect was also observed with TMP in high glucose-treated bEnd.3 (0.58 ± 0.09 *vs.* 1.13 ± 0.11, $P<0.01$), HUVEC (0.34 ± 0.12 *vs.* 0.93 ± 0.12, $P<0.05$) and HAEC (0.62 ± 0.05 *vs.* 0.84 ± 0.07, $P<0.05$) cells (Fig. 4B).

Involvement of UCP2 in antioxidant actions elicited by QHYH and TMP

Previous studies have proposed a role for UCP2 in controlling mitochondrial ROS production, and thus, the redox state and oxidative

stress of endothelial cells (Duval et al. 2002). Here, we detected a dose- and time-dependent suppression of endothelial UCP2 mRNA levels by high glucose concentrations using the real-time PCR method (Fig. 5A and B). Incubation with 35 mM D-glucose for 48 h down-regulated UCP2 mRNA in bEnd.3 cells by approximately 46% compared to untreated controls. This inhibition was accompanied by a decrease in UCP2 protein expression. QHYH or TMP treatment restored the UCP2 mRNA and protein levels to a state close or within the normal range (Fig. 5C and D).

To specifically address the role UCP2 played in suppression of ROS production by QHYH, we applied RNAi techniques to inhibit UCP2 protein expression. As shown in Fig. 6A, B and C, application of UCP2 siRNA caused an increase in ROS production ($P<0.001$) and a decrease in NO generation ($P<0.001$), Akt phosphorylation ($P<0.01$) and eNOS phosphorylation ($P<0.001$) in normal glucose medium, demonstrating that endogenous UCP2 expression is important for oxidation–reduction equilibrium and thus NO generation in bEnd.3 cells; the differences in high glucose were not statistically significant suggesting UCP2 expression had been highly suppressed in this environment prior to the siRNA treatment; when QHYH was added to the UCP2 siRNA treated bEnd.3 cells, its antioxidant effect against high glucose was partially abolished, resulting in a relative higher ROS production ($P<0.05$) and markedly diminished NO generation ($P<0.05$), Akt phosphorylation ($P<0.01$) and eNOS phosphorylation ($P<0.001$) in the presence of high glucose.

In order to confirm the above observations, we examined the effects of TMP in all the three types of endothelial cells. First, TMP was able to restore both UCP2 mRNA and protein levels in bEnd.3 cells under high glucose (from 0.61 ± 0.03 to 1.13 ± 0.07, $P<0.001$ and from 0.11 ± 0.05 to 0.63 ± 0.17, $P<0.01$, respectively; Fig. 5C and D). Similar UCP2 protein profiles were obtained with HUVEC and HAEC cells (from 0.24 ± 0.10 to 0.99 ± 0.17, $P<0.001$ and from 0.35 ± 0.07 to 0.86 ± 0.13, $P<0.01$, respectively; Fig. 5D). When UCP2 RNAi technology was employed, the inhibitory action of TMP on high glucose-induced ROS production was attenuated leading to a 1.53-fold increase from the basal level (before RNAi, $P<0.001$; Fig. 6A). Likewise, the effect of TMP on NO generation, phosphorylation of Akt and eNOS under high glucose was significantly blocked by transfection of UCP2 siRNAs in bEnd.3 cells ($P<0.01$ and $P<0.001$; Fig. 6B and C).

Discussion

Qing Huo Yi Hao (QHYH) is an herbal remedy derived from TCM, consisting of eight commonly used medicinal materials including *Ligusticum chuanxiong*, *Hirude nipponica*, *Astragalus membranaceus*, *Pueraria lobata*, *Gardenia jasminoides*, *Artemisia capillaries*, *Pteris multifida* and *Pericarpium Citri*. In this study, we examined the antioxidant effect of QHYH and its active components on oxidative stress induced by high glucose in three types of endothelial (bEnd.3, HUVEC and HAEC) cells. Among the 28 compounds isolated from QHYH, 11 active components were found to possess antioxidant properties. Since one of these, tetramethylpyrazine (TMP), displayed a consistent inhibitory effect on high glucose-induced ROS production, it was chosen for subsequent studies in parallel with QHYH. Treatment with QHYH or TMP was able to reverse the effects of high glucose on ROS production, eNOS/Akt phosphorylation, NO generation, and UCP2 mRNA/protein levels. When UCP2 expression was blocked by specific siRNAs, the antioxidant action of QHYH and TMP against high glucose was significantly abolished.

The vascular endothelial cell is an important target for hyperglycemic damage. Oxidative stress induced by high glucose leads to endothelial dysfunction, which is highly relevant to the pathology of diabetic vascular complications. Reduced production of NO and increased secretion of endothelin-1 are the two characteristic features of endothelial dysfunction (Lele 2007; Böhm and Pernow 2007). It has been reported that ROS may decrease NO content, thereby reducing the efficacy of the endothelium-derived vasodilator system involved in the homeostasis of the vasculature (O'Donnell and Freeman 2001; Benz et al. 2002). Our finding that high glucose decreased NO production in endothelial (bEnd.3, HUVEC and HAEC) cells is consistent with that described previously (Kimura et al. 2001; Ding et al. 2004). Reduction of high glucose-induced ROS production, extinguishing oxidants at the formation stage and restoration of NO generation are the key effects of QHYH and TPM observed in the present study, suggesting that they are protective against hyperglycemic environment and capable of mitigating oxidative stress related damage to endothelial cells.

In endothelial cells, NO is synthesized from the substrate L-arginine via endothelial NO synthase (eNOS). Endothelial NO production is predominantly regulated by eNOS. The phosphorylation of eNOS at residue Ser-1177 has important implications for its enzymatic activity (Yang and Ming 2006). Akt is the upstream kinase of eNOS and phosphorylation of Akt Ser-473 is correlated to the phosphorylation and activation of eNOS (Ser-1177) (Michell et al. 1999). We observed that high glucose treatment inhibited Akt activity and eNOS (Ser-1177) phosphorylation in endothelial cells. The situation was reversed following addition of QHYH or TMP indicating that both could increase endothelial NO production by activating the Akt/eNOS pathway. At this stage, it remains unclear about the correlation between inhibition of ROS production and activation of the Akt/eNOS pathway in endothelial cells, and this will be the focus of future investigations.

We have previously conducted a single-blind, randomized clinical trial in type 2 diabetic patients ($n=71$) to evaluate the effect of QHYH on UAER (urine albumin excreting rate). Following 24-week administration, the treated group showed an average decrease of 3.8 mg/24 h in UAER ($P=0.001$); the median level of UAER in 14 patients, whose baseline UAER was higher than 30 mg/24 h, was reduced by 36.2 mg/24 h after treatment ($P=0.001$); microcirculatory flow score, loop circumambience score and the total score of the treated group also decreased significantly ($P=0.001$, $P=0.020$ and $P=0.007$, respectively) (Yu et al. 2004). In addition, EPR (electron paramagnetic resonance) determination revealed that QHYH could extinguish: (i) 82.5% of the radicals produced in the hydroxyl radical generating model system (Zhang et al. 2005) and (ii) superoxide anion generated by endothelial cells cultured in high glucose milieu (Gao and Zhang 2007). These experimental and clinical observations indicate that QHYH is capable of extinguishing free radicals in endothelial cells, improving UAER, and increasing microcirculatory nail bed flow in type 2 diabetic patients. Consistent with the findings described in this paper, QHYH may be useful as a causal treatment for vascular oxidative stress.

UCP2 is a member of the mitochondrial anion transporter family, located at the internal membrane of the mitochondria and has the ability to dissociate oxidative respiration from ATP generation and to collapse the proton gradient across the inner mitochondrial membrane (Duval et al. 2002; Argiles et al. 2002). It was reported that UCP2 over-expression led to a significant increase in eNOS and a suppression of ROS production in HAEC cells (Lee et al. 2005). Over-expression of UCP2 also attenuated free radical production and oxidative damage mediated by FFA-induced activation of NF-κB (Brand and Esteves 2005). In the present study, we found that high glucose inhibited UCP2 mRNA expression in a time- and dose-dependent manner; QHYH and TMP restored both UCP2 mRNA and protein levels towards the normal state under hyperglycemic environment in endothelial cells. These findings, in combination with the result that QHYH and TMP attenuated high glucose-induced ROS production, suggest that QHYH and TMP may exert their antioxidant action by modulation of UCP2 expression. To test the hypothesis, we suppressed UCP2 expression in bEnd.3 cells by RNA interference. When UCP2 expression was blocked, the inhibitory effects of QHYH and TMP on high glucose-induced ROS production was lifted, implying that the action elicited by QHYH and TMP on endothelial ROS production may be mediated through UCP2.

The high glucose concentrations (25–35 mM) used in this study are not present in well-controlled diabetic patients, but might be seen in poorly controlled or new-onset diabetic populations. In certain stress conditions, such as ketoacidosis, hyperglycemic hyperosmolar state, inflammation or infection, extremely high glucose levels are also noted (Balasubramanyam et al. 1999; Chiasson et al. 2003). Thus, the findings of the present study may have some clinical relevance.

Conclusion

In summary, the herbal remedy QHYH and at least one of its active constituents, TMP, are protective against detrimental consequences of high glucose on ROS production, eNOS/Akt phosphorylation, and NO generation. The underlying mechanism of such an action may be partially related to increases in UCP2 mRNA/protein expression as demonstrated by RNAi experiments. These results point to a therapeutic potential of QHYH and TMP in the treatment of diabetic vascular complications.

Acknowledgements

We are indebted to L. Zhou and C. Zhou for valuable discussions. This work was supported in part by grants from the Ministry of Education of China (2006-024-6076 to XG), the Ministry of Science and Technology of China (2004CB518902 to MWW) and Shanghai Municipality government (07JC14011 to XG; 07DZ22920 to MWW).

References

Argiles JM, Busquets S, Lopez-Soriano FJ. The role of uncoupling proteins in pathophysiological states. Biochemical and Biophysical Research Communications 293 (4), 1145–1152, 2002.

Balasubramanyam A, Zern JW, Hyman DJ, Pavlik V. New profiles of diabetic ketoacidosis: type 1 vs. type 2 diabetes and the effect of ethnicity. Archives of Internal Medicine 159 (19), 2317–2322, 1999.

Basta G, Lazzerini G, Del Turco S. At least 2 distinct pathways generating reactive oxygen species mediate vascular cell adhesion molecule-1 induction by advanced glycation end products. Arteriosclerosis, Thrombosis, and Vascular Biology 25 (7), 1401–1407, 2005.

Benz D, Cadet P, Mantione K, Zhu W, Stefano GB. Tonal nitric oxide and health: a free radical and scavenger of free radicals. Medical Science Monitor: International Medical Journal of Experimental and Clinical Research 8 (1), RA1–RA4, 2002.

Böhm F, Pernow J. The importance of endothelin-1 for vascular dysfunction in cardiovascular disease. Cardiovascular Research 76 (1), 8–18, 2007.

Brand MD, Esteves TC. Physiological functions of the mitochondrial uncoupling proteins UCP2 and UCP3. Cell Metabolism 2 (2), 85–93, 2005.

Cave AC, Brewer AC, Narayanapanicker A, Ray R, Grieve DJ, Walker S, Shah AM. NADPH oxidases in cardiovascular health and disease. Antioxidants & Redox Signaling 8 (5–6), 691–728, 2006.

Ceriello A. New insights on oxidative stress and diabetic complications may lead to a "causal" antioxidant therapy. Diabetes Care 26 (5), 1589–1596, 2003.

Chevillotte E, Giralt M, Miroux B, Ricquier D, Villarroya F. Uncoupling protein-2 controls adiponectin gene expression in adipose tissue through the modulation of reactive oxygen species production. Diabetes 56 (4), 1042–1050, 2007.

Chiasson JL, Aris-Jilwan N, Bélanger R, Bertrand S, Beauregard H, Ekoé JM, Fournier H, Havrankova J. Diagnosis and treatment of diabetic ketoacidosis and the hyperglycemic hyperosmolar state. Canadian Medical Association Journal 168 (7), 859–866, 2003.

Cooper ME, Johnston CI. Optimizing treatment of hypertension in patients with diabetes. Journal of the American Medical Association 283 (24), 3177–3179, 2000.

Ding QF, Hayashi T, Packiasamy AR, Miyazaki A, Fukatsu A, Shiraishi H, Nomura T, Iguchi A. The effect of high glucose on NO and O_2^- through endothelial GTPCH1 and NADPH oxidase. Life Sciences 75 (26), 3185–3194, 2004.

Duval C, Negre-Salvayre A, Dogilo A, Salvayre R, Penicaud L, Casteilla L. Increased reactive oxygen species production with antisense oligonucleotides directed against uncoupling protein 2 in murine endothelial cells. Biochemistry and Cell Biology 80 (6), 757–764, 2002.

Eckel RH, Wassef M, Chait A, Sobel B, Barrett E, King G, Lopes-Virella M, Reusch J, Ruderman N, Steiner G, Vlassara H. Prevention conference VI: diabetes and cardiovascular disease: writing group II: pathogenesis of atherosclerosis in diabetes. Circulation 105 (18), e138–e143, 2002.

Gao X, Zhang B. The eliminating effects of a prescribed traditional Chinese medicine preparation on endothelium derived superoxide anion and its molecular mechanism. 43rd EASD Annual Meeting, Amsterdam, The Netherlands, September 18–21, 2007. Diabetologia, vol. 50, p. s480. Suppl.

Itoh Y, Ma FH, Hoshi H, Oka M, Noda K, Ukai Y. Determination and bioimaging method for nitric oxide in biological specimens by diaminofluorescein fluorometry. Analytical Biochemistry 287 (2), 203–239, 2000.

Jay D, Hitomi H, Griendling KK. Oxidative stress and diabetic cardiovascular complications. Free Radical Biology & Medicine 40 (2), 183–192, 2006.

Kimura C, Oike M, Koyama T, Ito Y. Impairment of endothelial nitric oxide production by acute glucose overload. American Journal of Physiology. Endocrinology and Metabolism 280(1), E171–E178, 2001

Kobayashi T, Matsumoto T, Kamata K. The PI3-K/Akt pathway: roles related to alterations in vasomotor responses in diabetic models. Journal of Smooth Muscle Research 41 (6), 283–302, 2005.

Kojima H, Urano Y, Kikuchi K, Higuchi T, Hirata Y, Nagano T. Fluorescent indicators for imaging nitric oxide production. Angewandte Chemie 38 (21), 3209–3212, 1999.

Lee KU, Lee IK, Han J, Song DK, Kim YM, Song HS, Kim HS, Lee WJ, Koh EH, Song KH, Han SM, Kim MS, Park IS, Park JY. Effects of recombinant adenovirus-mediated uncoupling protein 2 overexpression on endothelial function and apoptosis. Circulation Research 96 (11), 1200–1207, 2005.

Lele RD. Causation, prevention and reversal of vascular endothelial dysfunction. Journal of the Association of Physicians of India 55, 643–651, 2007.

Livak KJ, Schmittgen TD. Analysis of relative gene expression data using real-time quantitative PCR and the 2(-Delta Delta C(T)) method. Methods 25 (4), 402–408, 2001.

Michell BJ, Griffiths JE, Mitchelhill KI, Rodriguez-Crespo I, Tiganis T, Bozinovski S, de Montellano PR, Kemp BE, Pearson RB. The Akt kinase signals directly to endothelial nitric oxide synthase. Current Biology 9 (15), 845–848, 1999.

Newsholme P, Haber EP, Hirabara SM, Rebelato ELO, Procopio J, Morgan D, Oliveira-Emilio HC, Carpinelli AR, Curi R. Diabetes associated cell stress and dysfunction: role of mitochondrial and non-mitochondrial ROS production and activity. Journal of Physiology 583 (Pt1), 9–24, 2007.

Nishikawa T, Edelstein D, Du XL, Yamagishi S, Matsumura T, Kaneda Y, Yorek MA, Beebe D, Oates PJ, Hammes HP, Giardino I, Brownlee M. Normalizing mitochondrial superoxide production blocks three pathways of hyperglycaemic damage. Nature 404 (6779), 787–790, 2000.

O'Donnell VB, Freeman BA. Interactions between nitric oxide and lipid oxidation pathways: implications for vascular disease. Circulation Research 88 (1), 12–21, 2001.

Paravicini TM, Touyz RM. NADPH oxidases, reactive oxygen species, and hypertension: clinical implications and therapeutic possibilities. Diabetes Care 31 (Suppl 2), S170–S180, 2008.

Strijdom H, Muller C, Lochner A. Direct intracellular nitric oxide detection in isolated adult cardiomyocytes: flow cytometric analysis using the fluorescent probe, diaminofluorescein. Journal of Molecular and Cellular Cardiology 37 (4), 897–902, 2004.

Su J, Lucchesi PA, Gonzalez-Villalobos RA, Palen DI, Rezk BM, Suzuki Y, Boulares HA, Matrougui K. Role of advanced glycation end products with oxidative stress in resistance artery dysfunction in type 2 diabetic mice. Arteriosclerosis, Thrombosis, and Vascular Biology 28 (8), 1432–1438, 2008.

Teshima Y, Akao M, Jones SP, Marban E. Uncoupling protein-2 overexpression inhibits mitochondrial death pathway in cardiomyocytes. Circulation Research 93 (3), 192–200, 2003.

Yamagishi S, Matsui T, Nakamura K, Inoue H, Takeuchi M, Ueda S, Okuda S, Imaizumi T. Olmesartan blocks inflammatory reactions in endothelial cells evoked by advanced glycation end products by suppressing generation of reactive oxygen species. Ophthalmic Research 40 (1), 10–15, 2008.

Yang Z, Ming XF. Recent advances in understanding endothelial dysfunction in atherosclerosis. Clinical Medicine & Research 4 (1), 53–65, 2006.

Yu DQ, Li XM, Li X, Teng Y, Zhang JZ, Zhao NQ, Gao X. Effect and safety of a traditional Chinese medicine prescription on urine albumin excreting rate in type 2 diabetic patients. Shanghai Medical Journal 27 (7), 466–469, 2004.

Zhang B, Gao X, Li X. Antioxidant capacity of a prescribed Chinese traditional medicine preparation and its effects on microvascular endothelial cells in high glucose milieu. 41st EASD Annual Meeting, Athens, Greece, September 10–15, 2005. Diabetologia, vol. 48, p. A289. Suppl.